J. Fluid Mech. (1984), *vol.* 141, *pp.* 289–308
Printed in Great Britain

Wave propagation in a thin-walled liquid-filled initially stressed tube

By G. D. C. KUIKEN
Laboratory for Aero- and Hydrodynamics, Department of Mechanical Engineering, Delft University of Technology, The Netherlands

(Received 19 April 1982 and in revised form 20 December 1983)

Wave propagation through a thin-walled cylindrical orthotropic viscoelastic initially stressed tube filled with a Newtonian fluid is discussed. Special attention is drawn to the influence of the initial stretch on the wave propagation. It is shown that initial stretching of real arteries enhances the propagation of blood pressure pulses in mammalian arteries. The dispersion equation for the initial-value problem of a semi-infinite tube is also derived. It is shown that the speed of propagation and the attenuation vary with the distance from the support. The results obtained for the axial wave mode provide an explanation for the experimental observations, which is not possible with the results obtained for the infinite tube.

1. Introduction

The problem of the propagation of waves through cylindrical tubes filled with a fluid has been studied over more than 150 years. It has interested researchers like Young (1808), Helmholtz (1863), Kirchhoff (1868) and Rayleigh (1896). Since then the subject has not lost its attraction, because the problem has bearings on many practical applications. The studies involved deal with the dynamic response of pressure-transmission lines, acoustic-delay lines, acoustic waveguides, water-hammer and pulsatile flow in plastic and rubber tubes used in many fields of industry, while medical researchers have long been interested in mechanical models to describe the pulse wave in blood vessels. The relevance of the theoretical aspects of pressure-wave propagation is well recognized in research on cardiovascular mechanics, cardiophony and atherogenesis. In modelling, any realistic model for the dynamic behaviour of blood vessels should include the effects of transmural pressure, axial stretch, and the orthotropy and viscoelasticity of the wall. However the author of this paper has found only a single contribution (Maxwell & Anliker 1968) where, for an isotropic tube filled with an inviscid liquid, the initial stresses are correctly included. In considering the blood flow through large arteries or the low-frequency flow of liquids through rubber or soft plastic tubes, the long-wavelength approximation can be applied. For flow through arteries it is seen to be valid *in vivo* (Pedley 1980; Kuiken 1984). Consequently, linearized equations of motion are used. Further, the membrane equations of linear shell theory are used to describe the motion of the wall, where the terms that account for the effects of the initial stresses can be obtained from the theory of buckling of thin-walled shells. The results obtained for the infinite tube reveals that the initial stresses observed in real arteries are favourable for the pulsatile flow in a number of aspects.

The problem of wave propagation through a semi-infinite tube is an initial-value problem. The results show that the speed of propagation and the attenuation, which are local properties, vary with the distance to the support of the tube. This dependence is introduced through the observation that the constitutive equation for the radial and axial displacement of the wall is an indirect constitutive equation (de Groot & Mazur 1962) and the fact that larger axial displacements are possible at larger distances from the fixed point. Indirect constitutive equations can result in unexpected physical phenomena, e.g. diffusion against the concentration gradient (Yaron & Gal-Or 1974). Also, in the initial-value problem of the semi-infinite tube unexpected results for the wave propagation are obtained, which disappear if the initial stretch is such that the constitutive equation for the radial displacement reduces to a direct constitutive equation. The infinite-tube results for the untethered tube predict for the Lamb mode, which is associated with the axial motions of the tube wall, that the axial wall displacements become unbounded for the circular frequency going to zero, while the semi-infinite tube results predict that the axial displacements are small for small values of the circular frequency. Finally the semi-infinite tube results for the axial mode give an explanation of the experimental findings of van Citters (1960), of Anliker, Ogden & Moritz (1968) and the remark of McDonald (1974) that sometimes the axial mode is observed and sometimes not.

2. Equations of motion and kinematic boundary conditions for the liquid

To describe the fully developed oscillatory flow in a straight circular tube, the cylindrical coordinates r, θ, x will be used, the x-axis chosen along the axis of the tube. For this tube flow the equations of motion for a Newtonian or a linear elastic fluid can be linearized if the axial velocity is small with respect to the speed of wave propagation of the pressure pulse. For a homogeneous liquid the linearized equations without body forces and the equation of continuity are respectively

$$\frac{\partial \boldsymbol{v}}{\partial t} = -\frac{1}{\rho}\operatorname{grad} p + \nu\,\Delta \boldsymbol{v}, \tag{2.1}$$

$$\operatorname{div} \boldsymbol{v} = 0, \tag{2.2}$$

where $\boldsymbol{v}$ denotes the velocity vector of the liquid motion, ρ the density of the liquid, p the pressure, ν the kinematic viscosity and Δ the Laplace operator. On taking the divergence of (2.1) and using (2.2), the equation for the pressure becomes

$$\Delta p = 0. \tag{2.3}$$

A general solution of (2.1)–(2.3) is obtained by a Fourier or Laplace analysis. Assuming that $\boldsymbol{v}$ and p vary harmonically in x and t, one term of the Fourier decomposition of the velocity $\boldsymbol{v}$ and the pressure p is given by

$$[\boldsymbol{v}, p] = [\hat{\boldsymbol{v}}(r), \hat{p}(r)]\exp\left\{\mathrm{i}\omega\left(t-\frac{x}{c}\right)\right\}, \tag{2.4}$$

where ω is a real constant denoting the circular frequency and c is the complex propagation velocity. The hat $\wedge$ is used to indicate the amplitude of a periodic or transient quantity. Substituting (2.4) into (2.3), an ordinary differential equation of Bessel type is obtained for the pressure. The solution, satisfying the condition that the pressure remains finite at $r = 0$, becomes

$$\hat{p}(r) = \hat{p}_0 J_0\left(\frac{\mathrm{i}\omega r}{c}\right) = \hat{p}_0\left\{1 + O\left(\frac{\omega r}{c}\right)^2\right\}, \tag{2.5}$$

where $\hat{p}_0$ is the reference pressure at $r = 0$ and the expansion of the zeroth-order Bessel function of the first kind $J_0(y)$ is used. The subscript 0 is used to indicate a reference value. Substituting (2.4) with (2.5) into (2.1), the particular solutions for the amplitudes for the components u and v in the x- and r-directions of the velocity become respectively

$$\hat{u}(r) = \frac{\hat{p}_0}{\rho c} J_0\left(\frac{\mathrm{i}\omega r}{c}\right) = \frac{\hat{p}_0}{\rho c}\left\{1 + O\left(\frac{\omega r}{c}\right)^2\right\}, \tag{2.6}$$

$$\hat{v}(r) = \frac{\hat{p}_0}{\rho c} J_1\left(\frac{\mathrm{i}\omega r}{c}\right) = \frac{\hat{p}_0}{\rho c}\frac{\mathrm{i}\omega r}{2c}\left\{1 + O\left(\frac{\omega r}{c}\right)^2\right\}, \tag{2.7}$$

where in (2.7) the expansion of the first-order Bessel function of the first kind $J_1(y)$ is used. The solutions (2.6), (2.7) satisfy the equation of continuity (2.2). In the long-wavelength approximation, that is $|\omega a/c|^2 \ll 1$, where a denotes the radius of the tube, only the first term in (2.5)–(2.7) remains, and in the Laplace operator the second derivative in the x-direction may be neglected. For axisymmetric flows the equations of motion in the x- and r-directions then reduce to

$$\left.\begin{aligned} \frac{\partial u}{\partial t} &= -\frac{1}{\rho}\frac{\partial p}{\partial x} + \nu\left(\frac{\partial^2 u}{\partial r^2} + \frac{1}{r}\frac{\partial u}{\partial r}\right), \\ \frac{\partial v}{\partial t} &= -\frac{1}{\rho}\frac{\partial p}{\partial r} + \nu\left(\frac{\partial^2 v}{\partial r^2} + \frac{1}{r}\frac{\partial v}{\partial r} - \frac{v}{r^2}\right). \end{aligned}\right\} \tag{2.8}$$

Substituting (2.4) into (2.8), an ordinary Bessel equation of zeroth order for $\hat{u}(r)$ and of first order for $\hat{v}(r)$ is obtained. The solution of (2.8), satisfying the conditions that the velocity remains finite at $r = 0$, becomes

$$\left.\begin{aligned} \hat{u}(r) &= \frac{\hat{p}_0}{\rho c_0}\left[k' + A(x)\,F_0\left(\frac{\mathrm{i}^{\frac{3}{2}}\alpha r}{a}\right)\right], \\ \hat{v}(r) &= \frac{\hat{p}_0}{\rho c_0}\frac{\mathrm{i}\omega a}{c_0}\,k'\left[\frac{k' r}{2a} + B(x)\,F_1\left(\frac{\mathrm{i}^{\frac{3}{2}}\alpha r}{a}\right)\right], \end{aligned}\right\} \tag{2.9}$$

where $F_0(\lambda y)$, $F_1(\lambda y)$ are the zeroth- and first-order members of the functions $F_n(\lambda y)$ defined by

$$F_n(\lambda y) = \frac{2^n n!\, J_n(\lambda y)}{\lambda^n J_0(\lambda)}. \tag{2.10}$$

In (2.10) $J_n(\lambda y)$ denotes the nth-order Bessel function of the first kind. In (2.9) c_0 is a scale for c, taken equal to the Moens–Korteweg (1878) wave velocity defined by

$$c_0 = (E_\theta h/2\rho a)^{\frac{1}{2}}, \tag{2.11}$$

where E_θ denotes the circumferential Young modulus and h the thickness of the orthotropic, linear viscoelastic wall. The reference velocity (2.11) represents the wave velocity of an inviscid liquid in a compliant tube. The dimensionless parameters k' and α in (2.9) are defined by

$$k' = \frac{c_0}{c}, \quad \alpha = a\left(\frac{\omega}{\nu}\right)^{\frac{1}{2}}. \tag{2.12}$$

Kuiken (1984) performed numerical calculations, where the solutions of the dispersion equation (see §4) obtained with the velocity profiles satisfying the full linearized Navier–Stokes equations for an incompressible fluid are compared with the solutions of the dispersion equation using the low-frequency approximation (2.9). The comparison yields that for the mode associated with the radial motions of the tube wall the low-frequency approximation can be applied if $\omega a/c < 0.2$. For arteries $c \approx 5$ m/s. The lowest maximum value of the frequency is obtained for the largest arteries. For the aorta, frequencies up to 15 Hz can still be applied without violating the low-frequency approximation. For the mode associated with the axial tube-wall motions the lowest maximum value of the frequency is obtained for the smallest arteries and is determined by the condition $\omega a/c < 10$. Within the long-wavelength approximation the intrinsic system property k' is assumed to be a slowly varying function of the axial coordinate. Using the equation of continuity (2.2), $B(x)$ in (2.9) becomes

$$B(x) = A(x) - \frac{c_0}{\mathrm{i}\omega k'}\frac{\mathrm{d}A}{\mathrm{d}x}. \tag{2.13}$$

The function $A(x)$ is to be determined by the boundary conditions. To the linearization of the equations of motion there correspond linear boundary conditions at the wall $r = a$. Denoting the axial displacement of the wall by ξ and the radial displacement of the wall by η, the linearized kinematic boundary conditions at the wall are

$$u|_{r=a} = \frac{\partial \xi}{\partial t}, \quad v|_{r=a} = \frac{\partial \eta}{\partial t}. \tag{2.14}$$

3. Equations of motion of the tube wall

For an axially loaded cylindrical shell the flexural rigidities are only important in describing the displacements, rotations and moments in the neighbourhood of the rigid supports of a tube, where the prescribed displacements may not be consistent with the displacements belonging to the membrane solution. At a distance of only a few diameters from the fixed point, the membrane solution can always be used (Moodie, Haddow & Tait 1982; Flügge 1973). The tube may be initially stressed with a longitudinal tension S per unit length along the circumference and a circumferential tension T per unit length in the axial direction. These stress resultants form then the basic system. It is a membrane system and it is uniform all over the shell. That the initially stretched tube is the reference configuration of the cylindrical shell and not the unstretched tube is overlooked by most authors dealing with wave propagation through initially stretched tubes (Atabek & Lew 1966; Atabek 1968; Flaud *et al.* 1974; Pedley 1980). Only Maxwell & Anliker (1968) have used the correct shell equations for an initially stressed tube; however, the fluid is assumed to be inviscid. To obtain the correct differential equations for the perturbation stresses s^+ and t^+, the theory of buckling of cylindrical shells can be applied. In the theory of buckling one is particularly concerned with constructions in a prestressed state. Flügge's (1973) equations are considered to be adequate for all possible buckling modes (Koiter 1966). The standard membrane equations of motion of the wall, supplemented with terms due to the prestress (given by Flügge 1973, p. 448) are

$$\rho_w h \frac{\partial^2 \xi}{\partial t^2} = \frac{\partial s^+}{\partial x} + X + S\frac{\partial^2 \xi}{\partial x^2} - \frac{T}{a}\frac{\partial \eta}{\partial x}, \tag{3.1a}$$

$$\rho_w h \frac{\partial^2 \eta}{\partial t^2} = -\frac{t^+}{a} + Y + S\frac{\partial^2 \eta}{\partial x^2} + \frac{T}{a}\frac{\partial \xi}{\partial x}, \tag{3.1b}$$

where ρ_w denotes the density of the wall, X the stresses exerted on the wall in the axial direction, and Y the stresses exerted on the wall in radial direction. The first three terms of (3.1) represent the standard membrane equations for cylindrical shells. The third term on the right-hand side of (3.1 *b*) shows that a longitudinal prestress contributes to the forces in the radial direction owing to the curvature of the shell element. The last term on the right-hand side of (3.1 *a*) shows that the deflection of the shell element tilts slightly, causing the circumferential prestress to produce forces in the axial direction. These contributions are also given correctly by Flaud *et al.* (1974). The terms $S\,\partial^2\xi/\partial x^2$ and $(T/a)\,\partial\xi/\partial x$ are obtained from equilibrium considerations in the initially stretched reference configuration of the tube. The stresses X and Y exerted on the wall are

$$X = -\mu\left[\frac{\partial u}{\partial r}+\frac{\partial v}{\partial x}\right]_{r=a} - M_1\frac{\partial^2\xi}{\partial t^2} - L_1\frac{\partial\xi}{\partial t} - Z_{11}\xi - Z_{12}\eta, \tag{3.2a}$$

$$Y = \left[p-2\mu\frac{\partial v}{\partial r}\right]_{r=a} - M_2\frac{\partial^2\eta}{\partial t^2} - L_2\frac{\partial\eta}{\partial t} - Z_{22}\eta - Z_{21}\xi, \tag{3.2b}$$

where the first terms represent the hydrodynamic forces exerted by the liquid on the wall, while the other terms represent the stresses exerted by the surrounding external material, modelled respectively by inertia, damping and stiffness terms (Atabek 1968; Rubinow & Keller 1971). The coefficients M_i, L_i and Z_{ij} $(i, j = 1, 2)$ represent respectively the additional mass, the frictional coefficient of a dashpot and the spring coefficient of the mechanical model of the external material per unit area. Rubinow & Keller (1971) did not consider terms with M_i and L_i, but they showed that $Z_{12} = Z_{21} = 0$ if Z_{ij} is constant, which we henceforth assume. In the long-wavelength approximation the second term in the square brackets may be neglected.

Finally the linear stress–strain relations, following Patel & Vaishnav (1972), Atabek (1968) and Pedley (1980), are

$$t^+ = B_{11}\frac{\eta}{a}+B_{12}\frac{\partial\xi}{\partial x}, \tag{3.3a}$$

$$s^+ = B_{21}\frac{\eta}{a}+B_{22}\frac{\partial\xi}{\partial x}, \tag{3.3b}$$

where

$$\left.\begin{aligned} B_{11} &= \frac{E_\theta h}{1-\sigma_\theta\sigma_x}, \quad B_{22} = \frac{E_x h}{1-\sigma_\theta\sigma_x}, \\ B_{12} &= \frac{E_\theta h\sigma_x}{1-\sigma_\theta\sigma_x} = B_{21} = \frac{E_x h\sigma_\theta}{1-\sigma_\theta\sigma_x}, \end{aligned}\right\} \tag{3.4}$$

with $E_\theta, \sigma_\theta, E_x, \sigma_x$ the complex Young modulus and Poisson ratio in the circumferential direction θ and the axial direction x respectively. From (3.4) it follows that $E_\theta\sigma_x = E_x\sigma_\theta$, and a ratio γ_e of principal values is introduced:

$$\gamma_e = \frac{E_x}{E_\theta} = \frac{\sigma_x}{\sigma_\theta}. \tag{3.5}$$

4. The dispersion equation for the infinite tube

In the infinite tube the axial motion of the tube wall is not prescribed at any point. In that case all variables are assumed to be proportional to $\exp\{i\omega(t-x/c)\}$. The function $A(x)$ in (2.9) and (2.13) then becomes a constant. From the available physiological data (Pedley 1980), the radial tethering forces in (3.2*b*) are small with respect to p; hence (3.2*b*) reduces to $Y = p$. Also the inertia term in (3.1*b*) can be neglected in that case, and (3.1*b*) becomes in the long-wavelength approximation

$$0 = -\frac{t^+}{a} + p + \frac{T}{a}\frac{\partial \xi}{\partial x}. \tag{4.1}$$

In the linear theory the wall displacements ξ and η are assumed to vary also proportionally to $\exp\{i\omega(t-x/c)\}$. By substitution of these exponential dependence, (4.1) yields, using (3.3*a*) for the amplitudes,

$$-\frac{ik' B'_{12}\omega a}{c_0}\hat{\xi} + B'_{11}\hat{\eta} - \frac{a\hat{p}_0}{\rho c_0^2} = 0. \tag{4.2}$$

Using (3.3*b*), (3.1*a*) becomes

$$\left\{B'_{22}k'^2 + \frac{K'_1}{\omega^2 a^2/c_0^2}\right\}\frac{\omega a}{c_0}\hat{\xi} + ik' B'_{21}\hat{\eta} + \frac{iF}{2}\frac{a\hat{p}_0 A}{\rho c_0^2} = 0. \tag{4.3}$$

The kinematic boundary conditions (2.14*a*) yield, using (2.9*a*),

$$(k' + A)\frac{a\hat{p}_0}{\rho c_0^2} = i\frac{\omega a}{c_0}\hat{\xi}, \tag{4.4}$$

and finally using (2.9*b*) with (2.13) gives for (2.14*b*)

$$(k'^2 + k' F A)\frac{a\hat{p}_0}{\rho c_0^2} = 2\hat{\eta}. \tag{4.5}$$

The four unknown amplitudes $\hat{\xi}$, $\hat{\eta}$, $\hat{p}_0$ and $\hat{p}_0 A$ satisfy the four homogeneous equations (4.2)–(4.5), where the various dimensionless parameters used are defined by

$$\left.\begin{aligned} K'_1 &= \frac{a}{\rho c_0^2}[Z_{11} + i\omega L_1 - \omega^2(M_1 + \rho_w h)], \\ B'_{11} &= \frac{B_{11}}{\rho a c_0^2}, \quad B'_{12} = \frac{B_{12} - T}{\rho a c_0^2}, \\ B'_{21} &= \frac{B_{21} - T}{\rho a c_0^2} = B'_{12}, \quad B'_{22} = \frac{B_{22} + S}{\rho a c_0^2}, \\ F &= F_1(i^{\frac{3}{2}}\alpha). \end{aligned}\right\} \tag{4.6}$$

In order to solve these homogeneous equations the determinant of their coefficients has to be zero. This yields the dispersion equation

$$k'^4(1-F)(B'_{11}B'_{22} - B'_{12}B'_{21}) + k'^2\left\{F(B'_{12} + B'_{21} - \tfrac{1}{2}B'_{11}) - 2B'_{22} + \left[\frac{K'_1}{\omega^2 a^2/c_0^2}\right]B'_{11}(1-F)\right\} + F - \frac{2K'_1}{\omega^2 a^2/c_0^2} = 0. \tag{4.7}$$

The expression (4.7) is equivalent to (2.38) of Pedley (1980, p. 92), where the coefficient K'_2 is neglected, consistent with Pedley (1980, p. 96). However, the coefficients B'_{ij} $(i, j = 1, 2)$ are completely different from those defined by Pedley, if T and S are not equal to zero. Pedley does not discuss the effect of initial stress on the wave propagation. Therefore, only his equation (2.25) and (2.37) should be revised, with no further consequences for the discussion in his chapter 2.2. The solution for the velocities and wall displacements are obtained from (2.9) and by solving (4.2), (4.3), yielding

$$\hat{u} = \frac{\hat{p}_0}{\rho c_0} k' \left[1 - m F_0 \left(\frac{\mathrm{i}^{\frac{3}{2}} \alpha r}{a} \right) \right], \tag{4.8}$$

$$\hat{v} = \frac{\hat{p}_0}{\rho c_0} \frac{\mathrm{i}\omega a}{c_0} \tfrac{1}{2} k'^2 \left[\frac{r}{a} - m F_1 \left(\frac{\mathrm{i}^{\frac{3}{2}} \alpha r}{a} \right) \right], \tag{4.9}$$

$$\frac{\hat{\eta}/a}{\hat{p}_0/\rho c_0^2} = \tfrac{1}{2} k'^2 (1 - mF). \tag{4.10}$$

$$\frac{\hat{\xi}/a}{\hat{p}_0/\rho c_0^2} = -\frac{\mathrm{i}k'(1-m)}{\omega a / c_0}, \tag{4.11}$$

where m is defined by:

$$m = \frac{2K + (2B'_{22} - B'_{21})\, k'^2}{2K - F + (2B'_{22} - B'_{21} F)\, k'^2}, \tag{4.12a}$$

$$K = \frac{K'_1}{\omega^2 a^2 / c_0^2}. \tag{4.12b}$$

In discussion of the effects of the initial stresses, asymptotic solutions of the dispersion equation will now bring out the qualitative features of increasing the initial stresses. The asymptotic expansions of F for large and small values of α are

$$F = \frac{2}{\alpha \mathrm{i}^{\frac{1}{2}}} \left[1 - \frac{1}{2\alpha \mathrm{i}^{\frac{1}{2}}} + O(\alpha^{-2}) \right] \quad \text{as} \quad \alpha \to \infty, \tag{4.13a}$$

$$F = 1 - \tfrac{1}{8}\mathrm{i}\alpha^2 - \tfrac{1}{48}\alpha^4 + O(\alpha^6) \quad \text{as} \quad \alpha \to 0. \tag{4.13b}$$

For $K'_1 = 0$ and $\alpha \to \infty$ the two roots of (4.7) are approximately

$$k_1'^2 = \frac{2B'_{22}}{B'} \left[1 + \left(\frac{2}{\alpha \mathrm{i}^{\frac{1}{2}}} \right) \left\{ \left(1 - \frac{B'_{21}}{2B'_{22}} \right)^2 + \frac{B'_{21}}{2B'_{22}} \right\} \right], \tag{4.14a}$$

$$k_2'^2 = (B'_{22} \alpha \mathrm{i}^{\frac{1}{2}})^{-1}, \tag{4.14b}$$

where

$$B' = B'_{11} B'_{22} - B'_{12} B'_{21}. \tag{4.15}$$

Writing (2.4) as

$$p = \hat{p}_0 \exp\left(-\frac{k_i x}{\lambda_i} \right) \exp\left\{ \mathrm{i}\omega \left(t - \frac{x}{c_i} \right) \right\}, \tag{4.16}$$

where $\lambda_i = 2\pi c_i/\omega$ is the wavelength of the ith mode of the wave, it follows that the phase velocity c_i and the attenuation or logarithmic decrement k_i of the ith mode of the wave are defined by

$$c_i = [\mathrm{Re}\,(k'/c_0)]^{-1}, \tag{4.17a}$$

$$k_i = -2\pi \frac{\mathrm{Im}\,(k'/c_0)}{\mathrm{Re}\,(k'/c_0)}. \tag{4.17b}$$

The phase velocity and attenuation calculated from (4.14a), representing the first mode or Young mode, are

$$c_1 = c_0 \left(\frac{B'}{2B'_{22}} \right)^{\frac{1}{2}} \left[1 - (2\alpha^2)^{\frac{1}{2}} \left\{ \left(1 - \frac{B'_{21}}{2B'_{22}} \right)^2 + \frac{B'_{21}}{2B'_{22}} \right\} \right], \tag{4.18a}$$

$$k_1 = \frac{2^{\frac{1}{2}}\pi}{\alpha} \left\{ \left(1 - \frac{B'_{21}}{2B'_{22}} \right)^2 + \frac{B'_{21}}{2B'_{22}} \right\}. \tag{4.18b}$$

The dimensionless tube parameters B'_{ij} from (4.6) and B' from (4.15) are given explicitly by

$$\left.\begin{aligned} B'_{11} &= \frac{2}{1-\gamma_e\sigma_\theta^2}, \quad B'_{22} = \frac{2(\gamma_e+S')}{1-\gamma_e\sigma_\theta^2}, \\ B'_{12} &= B'_{21} = \frac{2(\gamma_e\sigma_\theta - T')}{1-\gamma_e\sigma_\theta^2}, \\ B' &= \frac{4\{\gamma_e+S'-(\gamma_e\sigma_\theta-T')^2\}}{(1-\gamma_e\sigma_\theta^2)^2}, \end{aligned}\right\} \tag{4.19}$$

where the stretches S' and T' are defined by

$$S' = \frac{S}{\rho a c_0^2}, \quad T' = \frac{\hat{p}_{tm}}{\rho c_0^2}, \tag{4.20}$$

$\hat{p}_{tm}$ denoting the transmural pressure. For the isotropic wall $\gamma_e = 1$, involving $\sigma_\theta = \sigma$, and without initial stresses, (4.18) reduces to the result of Pedley (1980). From (4.18) with (4.19) we notice that the phase velocity and the small attenuation of this pressure wave increase with decreasing $\sigma_x - T'$. Hence, for a fixed value of σ_x an increase of the initial transmural pressure increases the phase velocity and the attenuation. If $T' = \sigma_x$ then $c_1 = c_0(1-\gamma\sigma_\theta^2)^{-\frac{1}{2}}$, and $m = 1 - B'_{21}/2B'_{22} + O(\alpha^{-1})$ becomes ≈ 1, whence there are no axial wall motions and the axial velocity profile reduces to that of a rigid tube. It is remarkable that, for an initial transmural pressure of 10^4 N m^{-2} ($\approx$ a diastolic pressure of 80 mmHg) and $c_0 \sim 5$ m s^{-1}, T' becomes ~ 0.4, which is of the order of the Poisson ratio of arteries. For $B'_{21} = 0$ the radial displacements $(\hat{\eta}/a)/(\hat{p}_0/\rho c_0^2) = 1/B'_{11}$ and become independent of α and k'. An increase in the longitudinal stretch increases also the phase velocity and the attenuation, but less than a comparable increase of the transmural pressure.

The second root of (4.7), (4.14*b*) represents the second mode or Lamb mode with an attenuation of $2\pi \tan\frac{1}{8}\pi \approx 2.6$ and a phase velocity $c_2 = c_0(B'_{22}\alpha)^{\frac{1}{2}} \sec\frac{1}{8}\pi$. Longitudinal stretch increases the wave speed, while the effect of a transmural pressure becomes negligible in the limit $\alpha \to \infty$. The principal wall motions for the second root are longitudinal, which follows from the ratio between (4.11) and (4.10), yielding $\hat{\xi}/\hat{\eta} = -2\mathrm{i}^{\frac{3}{2}}(B'_{22}\alpha)^{\frac{1}{2}}/(\omega a/c_0)$.

For $K'_1 = 0$ and $\alpha \to 0$ the two roots of (4.7) are approximately

$$k_1'^2 = \frac{8}{\mathrm{i}\alpha^2}\left\{\frac{4(B'_{22}-B'_{12})+B'_{11}}{2B'} + \frac{\mathrm{i}\alpha^2}{8}\left[\frac{4(4B'_{22}+3B'_{12})-3B'_{11}}{6B'} - \frac{2}{4(B'_{22}-B'_{12})+B'_{11}}\right]\right\}, \tag{4.21a}$$

$$k_2'^2 = \frac{2}{4(B'_{22}-B'_{12})+B'_{11}}\left[1 - \frac{\mathrm{i}\alpha^2}{6}\frac{3B'_{22}+B'_{11}-2B'_{12}}{4(B'_{22}-B'_{12})+B'_{11}}\right]. \tag{4.21b}$$

If $\gamma_e = 1$, $\sigma_\theta = \sigma$, $T' = S' = 0$ the result of Pedley (1980) is obtained. The first root represents the pressure wave with an attenuation $\approx 2\pi$ and a wave speed $c_1 = c_0\alpha[B'/\{8(B'_{22}-B'_{12})+2B'_{11}\}]^{\frac{1}{2}}$. Here the transmural pressure decreases the wave speed. For $\alpha \to 0$ Pedley (1980) and Lighthill (1970) discuss the fact that the first root does not really represent a pressure wave since inertia is negligible, and the phenomenon is more a diffusive one rather than a wave one. The second root (4.21*b*) shows no attenuation, and an increase of the transmural pressure as well as a longitudinal stress increases the wave speed. However, as $m \neq 1$ this root predicts extreme large longitudinal wall displacements, as follows from (4.11) with

$\omega a/c_0 = (\nu/ac_0)\alpha^2$ very small for $\alpha \ll 1$. This behaviour is a consequence of the fact that for an infinite tube no axial boundary conditions in some point of the tube are imposed. The large longitudinal wall displacements for $\alpha \to 0$ are not observed in reality and this is usually attributed to the hindrance of the axial wall displacements due to longitudinal tethering of the wall (Pedley 1980), but a single constraint at a point achieves the same, as will be discussed in §6.

For $K_1' \neq 0$ and $(\omega a/c_0)^2 \ll 1$, where α need not be small, the asymptotic solutions of (4.7) are approximately

$$k_1'^2 = 2/(1-F)\,B_{11}', \tag{4.22a}$$

$$k_2'^2 = -KB_{11}'/B'. \tag{4.22a}$$

For an isotropic wall (4.22*a*) is the solution given by Kerris (1939), Zwikker & Koster (1949) and Iberall (1950). In this solution the effects of the initial stresses are absent, and as $m = 1$ no axial wall motions occur. The approximate solutions (4.22) are also valid for $\alpha \to 0$. The dispersion equation (4.7) reduces with (4.13*b*) approximately to

$$k'^4B' + Kk'^2\left\{B_{11}' + \frac{8\omega^2a^2/c_0^2}{\alpha^2}\,\frac{2B_{21}' - \frac{1}{2}B_{11}' - 2B_{22}'}{K_1'}\right\} - \frac{16K}{\mathrm{i}\alpha^2} = 0. \tag{4.23}$$

Since $\omega a/c_0 = (\nu/ac_0)\alpha^2 \approx 10^{-4}\alpha^2$ for blood flow through the large arteries, the second term does not contribute for $\alpha \to 0$, as Pedley (1980) assumes, and (4.22) is again obtained.

Numerical solutions will confirm the above qualitative results. To compare these results with Atabek & Lew (1968), an isotropic elastic wall without tethering but with wall inertia will be considered. The same numerical values as those of Atabek & Lew will be used, namely $\sigma = 0.5$, $K = -0.1$, α varying between zero and 10, while S'/B_{11}' and T'/B_{11}' are varied between zero and 1. This means that very large initial deformations are involved. Large deformations are usually not consistent with linear theory. However, the reference configuration *is* the initially stretched tube and the linear theory is applied for the small perturbations with respect to this reference state.

The effects on the Young mode and the Lamb mode if the strains S' and T' are varied are displayed in figures 1–4. In figure 1 the effect is shown on the dimensionless phase velocity c_1/c_0 as a function of α for increasing values of T'. For the Young mode an increase of the phase velocity is shown for increasing values of the transmural pressure, up to strains of 50 %, when B_{21}' becomes zero. For a further increase the classical equations of elastic stability (Flügge 1973; Koiter 1966) predict a decrease of the phase velocity, although one would expect a monotonic behaviour, hence a further increase. A critical examination of the foundations of these equations is being undertaken by the author and will be reported in due time. Anyway, McDonald (1974, p. 407, figure 14.12) gives experimental results showing an increase of c_1/c_0 with increasing values of the transmural pressure. Therefore, although comparison with experiment is very hard since the elastic properties of biological tissue are nonlinear, the experiments and the above numerical results point in the same direction. It should be noted that Atabek & Lew (1966) find the opposite behaviour. The same figure shows that the phase velocities of the second mode, the Lamb mode, are much faster than those of the first mode, the Young mode. The phase velocity of the Lamb mode increases with the frequency parameter α and with the prestrain T'.

Figure 2 shows the effect of varying T' on the decrement $\exp(-k)$, termed the 'transmission per wavelength' by Atabek & Lew. For the Young mode a more significant effect is shown than shown by Atabek & Lew, while for the Lamb mode the opposite conclusion follows. The decrement behaviour with α is for the fast wave

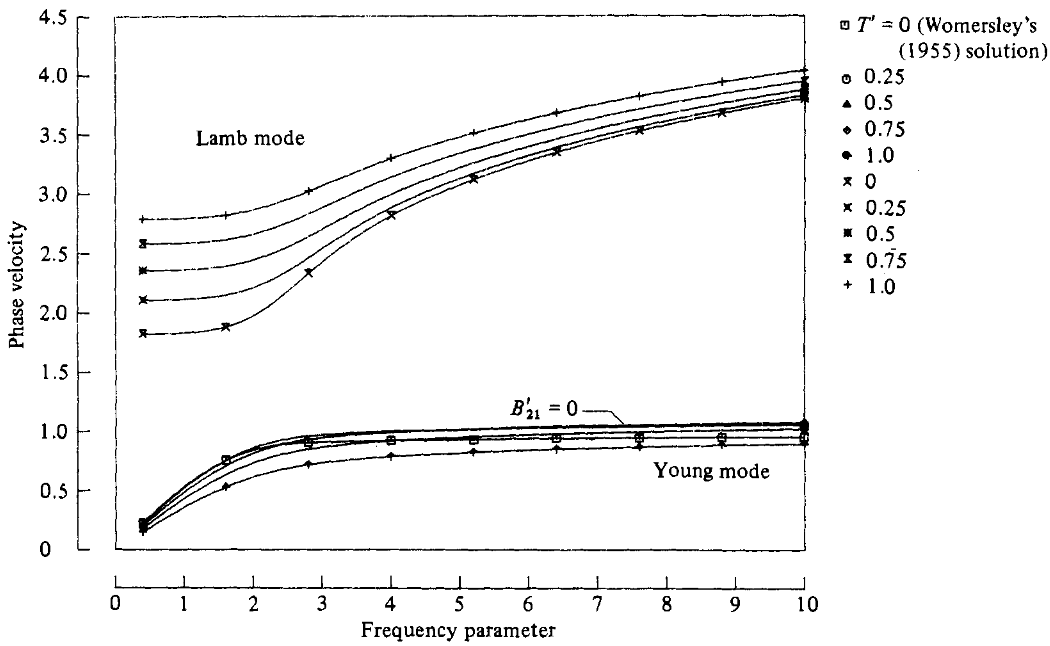

FIGURE 1. Dimensionless phase velocity of the Young mode and the Lamb mode as a function of the frequency parameter for various values of the circumferential prestrain T'.

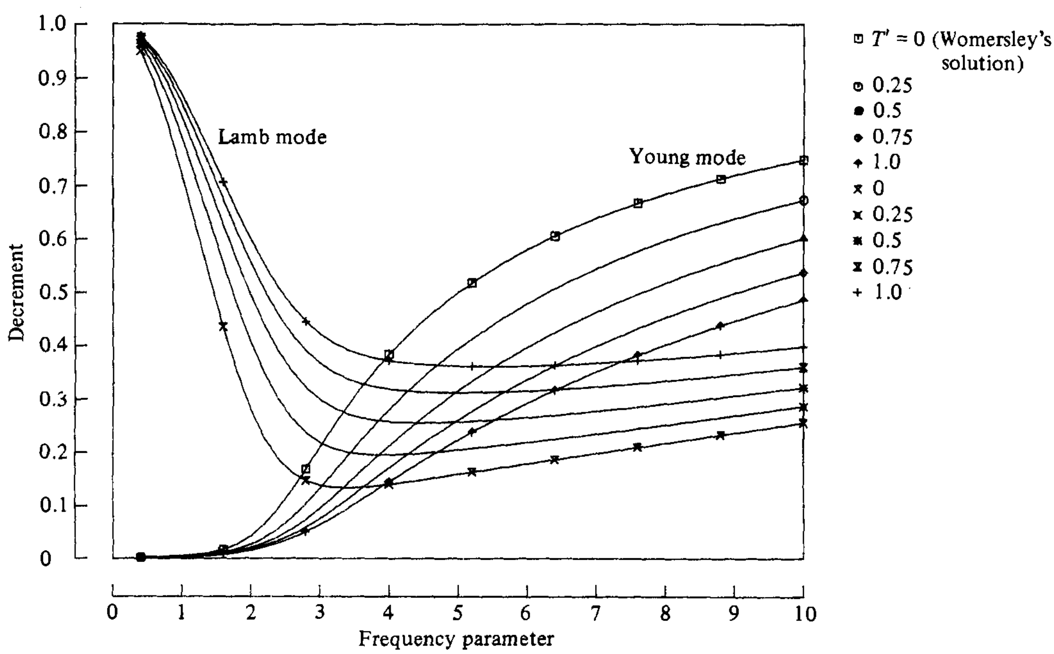

FIGURE 2. Decrement of the Young mode and the Lamb mode as a function of the frequency parameter for the same values as in figure 1.

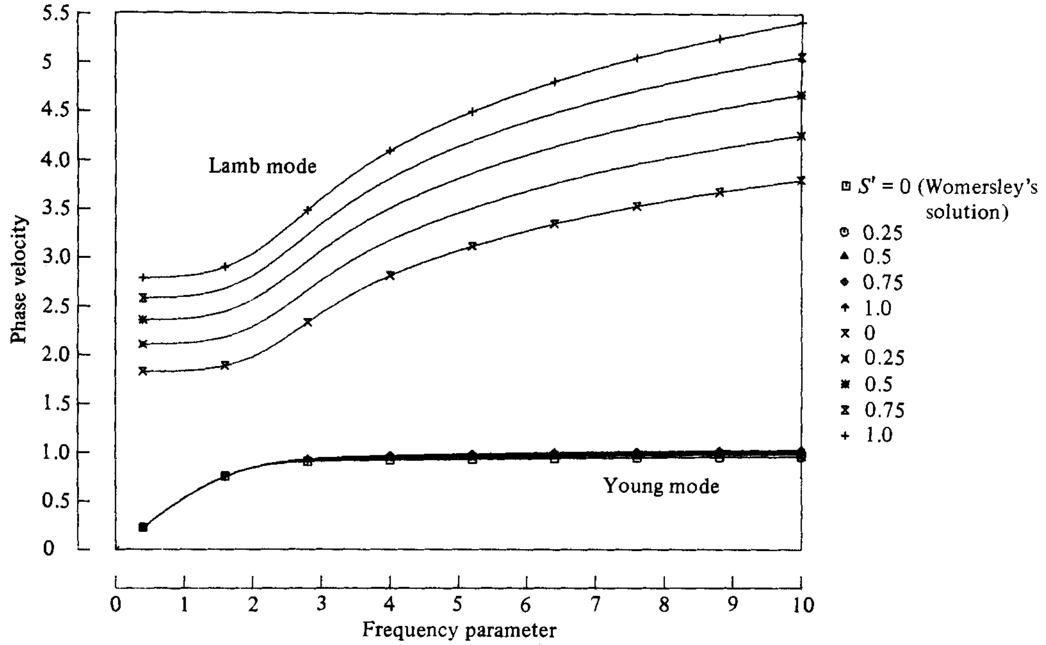

FIGURE 3. Dimensionless phase velocity of the Young mode and the Lamb mode as a function of the frequency parameter for various values of the longitudinal prestrain S'.

also quite different from that of the slow waves. For small values of α the slow wave is not propagating as the fast wave is. With increasing values of α the decrement of the slow wave is monotonically increasing, while for the fast wave it decreases rapidly, going through a minimum at α about 3 and then increasing slowly.

Figure 3 shows the effect on the phase velocity if the axial prestress is varied. For the Young mode the phase velocity increases only slightly with an increase of S'. This is also consistent with measurements reported by Flaud *et al.* (1975). For the Lamb mode the longitudinal strain S' has a considerable effect on the phase velocity. The tendency shown by the Lamb mode conforms with the pictures given by Atabek & Lew, although the variation with S' is much more pronounced.

Finally figure 4 shows the associated decrements if S' is varied. The variations in the decrements are moderate for both modes.

5. The dispersion equation for a semi-infinite tube

For a semi-infinite tube the axial displacement of the tube at $x = 0$ is assumed to be zero. The tube is axially fixed at that point. Such a configuration is obtained e.g. for an artery where the surrounding tissue is removed over some distance. For the tethered tube ($x \leqslant 0$) the axial displacements are zero, but for $x > 0$ the axial displacements are not hindered. Figure 5 shows the tube with its support at $x = 0$.

With the boundary condition shown in figure 5 the radial motion of the wall of the flexible tube can be followed at $x = 0$. The membrane equations are then sufficient and applicable from $x \geqslant 0$. If other boundary conditions are chosen, e.g. a rigid tube to which the flexible tube is attached, the flexural rigidities become important. However, for the axially symmetrically loaded cylindrical shell, the effects of other boundary conditions extend only over a small distance from the support. These effects

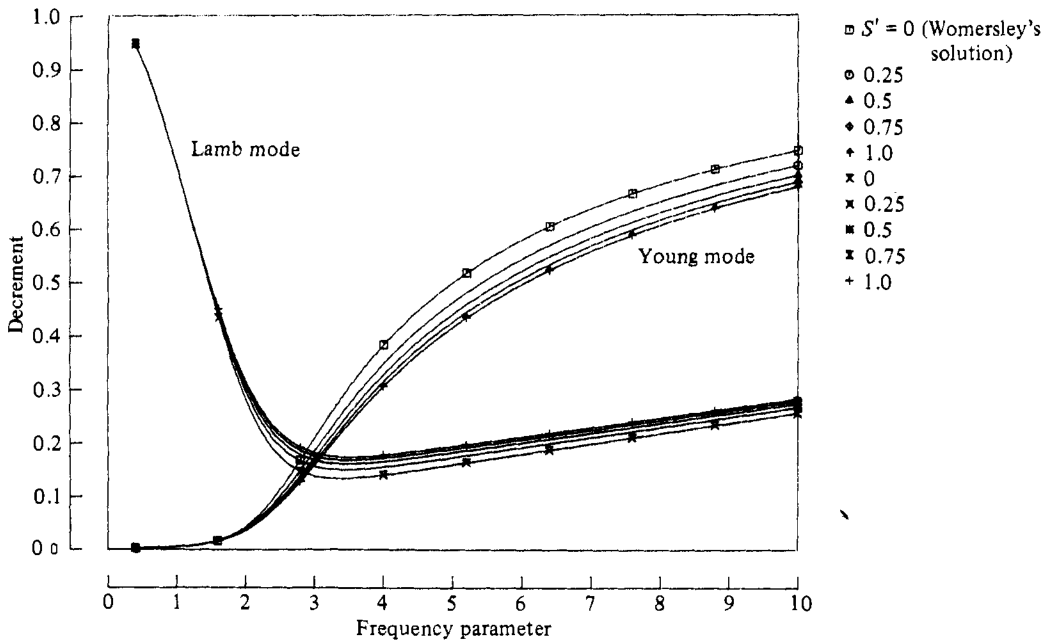

FIGURE 4. Decrement of the Young mode and the Lamb mode as a function of the frequency parameter for the same values as in figure 3.

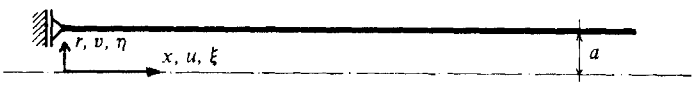

FIGURE 5. Axially supported semi-infinite tube.

can be neglected already at a distance of a few diameters from the support (Moodie *et al.* 1982). In this section particularly the effect of axial stretching, due to stresses exerted by the flow on the wall, is considered. As the relative displacement in axial direction with respect to the fixed point $x =$ increases with x it may be inferred that the influence of stretching becomes more dominant with increasing distance from the support. From (3.3) and (4.1) we have for the wall displacements:

$$\eta = \frac{B_{22} pa^2 - (B_{12} - T)\, s^+ a}{B_{11} B_{22} - B_{21}(B_{12} - T)}, \tag{5.1a}$$

$$\frac{\partial \xi}{\partial x} = \frac{-B_{21} pa + B_{11} s^+ a}{B_{11} B_{22} - B_{21}(B_{12} - T)}, \tag{5.1b}$$

where from the shell equation (3.1 a) it follows that

$$s^+ = \int_0^x \left(-X + \rho_w h \frac{\partial^2 \xi}{\partial t^2} - S \frac{\partial^2 \xi}{\partial x^2} + \frac{T}{a} \frac{\partial \eta}{\partial x} \right) \mathrm{d}x. \tag{5.2}$$

At this point it should be noted that the axial stresses influence the radial displacement η, as the second term on the right-hand side of (5.1 a) shows. From (5.2) it is noticed that η is now not simply proportional to $\exp\{i\omega(t - x/c)\}$, but it is assumed that η can be factorized with this term. The differences obtained with the classical results are mainly due to this term and for $B_{12}-T=0$ the results are comparable to the results for the unbounded tube.

For $x=0$ it follows that $s^+=0$ and $\xi=0$. From (5.1) we obtain the conditions at the support:

$$\eta=\frac{B_{22}pa^2}{B_{11}B_{22}-B_{21}(B_{12}-T)}, \tag{5.3a}$$

$$\frac{\partial\xi}{\partial x}=-\frac{B_{21}pa}{B_{11}B_{22}-B_{21}(B_{12}-T)} \quad (x=0, \quad r=a). \tag{5.3b}$$

For the whole tube the kinematic boundary conditions (2.14) are applicable. Substitution of (5.2) into (5.1*b*), execution of the integration of (5.2) with (5.3) and using the kinematic boundary condition, $u=\partial\xi/\partial t$, an integral equation for u at $r=a$ is obtained:

$$\rho ac_0^2 u=\frac{B'_{11}}{B'}\int_0^x\int_0^x\left\{\mathrm{i}\omega\mu\frac{\partial u}{\partial r}+K'_1\left(\frac{\rho c_0^2}{a}\right)u\right\}\mathrm{d}x^2-\frac{B'_{21}}{B'}\mathrm{i}\omega a\int_0^x p\,\mathrm{d}x-\frac{B'_{TS}B'_{11}}{B'}\mathrm{i}\omega axp\bigg|_{x=0}. \tag{5.4}$$

Differentiation of (5.4) yields the differential equation

$$\rho ac_0^2\frac{\partial^2 u}{\partial x^2}=\frac{B'_{11}}{B'}\left\{\mathrm{i}\omega\mu\frac{\partial u}{\partial r}+K'_1\left(\frac{\rho c_0^2}{a}\right)u\right\}-\frac{B'_{21}}{B'}\mathrm{i}\omega a\frac{\partial p}{\partial x}, \tag{5.5}$$

with two boundary conditions at $x=0$, $r=a$ respectively

$$u|_{x=0}=0, \quad \rho ac_0^2\frac{\partial u}{\partial x}\bigg|_{x=0}=-\frac{B'_{21}+B'_{TS}B'_{11}}{B'}\mathrm{i}\omega ap\bigg|_{x=0}, \tag{5.6}$$

where B'_{TS} is defined by:

$$B'_{TS}=\frac{B'_{22}T'+B'_{21}S'}{B'-B'_{11}S'-B'_{12}T'}. \tag{5.7}$$

The radial motion of the wall $x=0$ is chosen to be consistent with the membrane solution. The effect of the prestresses for the semi-infinite tube is different from the infinite tube owing to the conditions at $x=0$. The difference is already manifested through the dimensionless quantity B'_{TS}, which does not occur for the infinite tube. The unknown function $\hat{p}_0A(x)$ is found from (5.6) when u and p are substituted from (2.9*a*) and (2.4*b*) respectively. The solution is given by

$$\hat{p}_0A(x)=\hat{p}_0A_1\exp\left\{\frac{\mathrm{i}\omega a}{c_0}\frac{x}{a}(k'+\delta_1)\right\}+\hat{p}_0A_2\exp\left\{\frac{\mathrm{i}\omega a}{c_0}\frac{x}{a}(k'-\delta_1)\right\}+\hat{p}_0A_p, \tag{5.8}$$

with $\hat{p}_0A_p$ satisfying

$$\hat{p}_0A_p(k'^2-\delta_1^2)+\hat{p}_0(k'^2-\delta_2^2)\,k'=0, \tag{5.9}$$

where δ_1 and δ_2 are dimensionless parameters defined by:

$$\delta_1^2=-\frac{B'_{11}K}{B'}+\frac{B'_{11}F}{2B'}, \tag{5.10a}$$

$$\delta_2^2=-\frac{B'_{11}K}{B'}+\frac{B'_{21}}{B'}. \tag{5.10b}$$

Substitution of (5.8) into (2.9) yields for the axial velocity

$$u=\frac{\hat{p}_0}{\rho c_0}\left\{\left[k'+A_pF_0\left(\frac{\mathrm{i}^{\frac{3}{2}}\alpha r}{a}\right)\right]\exp\mathrm{i}\omega\left(t-\frac{x}{c}\right)\right.$$
$$\left.+F_0\left(\frac{\mathrm{i}^{\frac{3}{2}}\alpha r}{a}\right)\left[A_1\exp\mathrm{i}\omega\left(t+\frac{\delta_1x}{c_0}\right)+A_2\exp\mathrm{i}\omega\left(t-\frac{\delta_1x}{c_0}\right)\right]\right\}. \tag{5.11}$$

and for the radial velocity

$$v = \frac{\mathrm{i}\omega a\hat{p}_0}{2\rho c_0^2}\left\{k'\left[\frac{k'r}{a}+A_p F_1\left(\frac{\mathrm{i}^{\frac{3}{2}}\alpha r}{a}\right)\right]\exp \mathrm{i}\omega\left(t-\frac{x}{c}\right) + F_1\left(\frac{\mathrm{i}\alpha^{\frac{3}{2}}r}{a}\right)\left[-\delta_1 A_1 \exp \mathrm{i}\omega\left(t+\frac{\delta_1 x}{c_0}\right)+\delta_1 A_2 \exp \mathrm{i}\omega\left(t-\frac{\delta_1 x}{c_0}\right)\right]\right\}. \quad (5.12)$$

For the tethered tube $x \leqslant 0$ it is justifiable to assume that the pressure can be written as $\hat{p}_0 \exp\{\mathrm{i}\omega(t-x/c)\}$. This Fourier term of the pressure is associated with an 'incident' wave propagating towards $x = 0$ from $-\infty$, where the axial displacements go continuously over in the non-zero displacements of the untethered tube. The velocity profiles for $x = 0$ show a term propagating upstream with wave speed $c_0/|\mathrm{Re}\,(\delta_1)|$. This is a non-propagating wave for the tethered tube, since, for $\alpha \to 0$, $K = K_1'/(\omega^2 a^2/c_0^2)$ is very large, whereas, for $\alpha \to \infty$, $F = 0$ and from (5.10a) it follows that $\delta_1 \to \mathrm{i}(B_{11}' K/B')^{\frac{1}{2}}$. It is obvious from (5.11) and (5.12) that every variable proportional to $\exp \mathrm{i}\omega(t-x/c)$ no longer applies to the semi-infinite tube. The two unknown constants $\hat{p}_0 A_1$ and $\hat{p}_0 A_2$ are determined by the two conditions (5.6) at $x = 0$, yielding
determined by the two conditions (5.6) at $x = 0$, yielding

$$\hat{p}_0 A_1 + \hat{p}_0 A_2 + \hat{p}_0 A_p + \hat{p}_0 k' = 0, \quad (5.13)$$

$$-\delta_1 k' \hat{p}_0 A_1 + \delta_1 k' \hat{p}_0 A_2 + \delta_1^2 \hat{p}_0 A_p - (K + B_{TS}')(B_{11}'/B')\hat{p}_0 k' = 0. \quad (5.14)$$

Finally two homogenous equations are obtained from the conditions in the radial direction: the kinematic boundary condition (2.14b) and the radial displacement (5.1a). For the determination of (5.1a) we have to evaluate the integral (5.2). Substituting (5.1) and X (3.2a) an integral equation in s^+ is obtained. The solution is found by differentiation analogous to (5.4). The solution procedure is straightforward but elaborate. Factorization of the radial wall displacement η in the form

$$\eta(x) = \hat{\eta}(x)\exp(\mathrm{i}\omega(t-x/c), \quad (5.15)$$

and substitution of the explicit expression for s^+ into (5.1a) yield the homogeneous equation

$$G(-\delta_1)\hat{p}_0 A_1 + G(\delta_1)\hat{p}_0 A_2 + G(k')\hat{p}_0 A_p + \frac{(B_{22}'-S')(1-\epsilon)}{B'-B_{11}'S'-B_{12}'T'}\hat{p}_0 a^2 - 2\rho a c_0^2 \hat{\eta} = 0. \quad (5.16)$$

In (5.16) the function G is defined by

$$G(y) = \frac{B_{12}' a^2 F\left[1-\exp\left(\frac{\mathrm{i}\omega x}{c}\right)\left\{1-\frac{\gamma}{y}\sinh\left(\frac{B_{11}'K_1'}{B'}\right)^{\frac{1}{2}}\frac{x}{a}\right\}\right]}{B' y(1-\gamma^2/y^2)},$$

where $\gamma^2 = -B_{11}' K/B'$, while the function ϵ is given by

$$\epsilon = \frac{B_{12}'}{B_{22}'-S'}\left(\frac{B_{22}'T'+B_{21}'S'}{B'} - \frac{B_{21}'+T'}{B_{11}'}\frac{\gamma^2}{k'^2}\right)\left(1-\frac{\gamma^2}{k'^2}\right)^{-1} \times\left[1-\exp\left(\frac{\mathrm{i}\omega x}{c}\right)\left\{1-\frac{\gamma}{k'}\sinh\left(\frac{B_{11}'K_1'}{B'}\right)^{\frac{1}{2}}\frac{x}{a}\right\}\right].$$

The kinematic boundary condition (2.14b) becomes, with (2.4), (5.12) and (5.15),

$$-\delta_1 a^2 F \hat{p}_0 A_1 \exp\left\{\frac{\mathrm{i}\omega a}{c_0}\frac{x}{a}(k'+\delta_1)\right\} + \delta_1 a^2 F \hat{p}_0 A_2 \exp\left\{\frac{\mathrm{i}\omega a}{c_0}\frac{x}{a}(k'-\delta_1)\right\} + k' a^2 F \hat{p}_0 A_p + k'^2 \hat{p}_0 a^2 - 2\rho a c_0^2 \hat{\eta} = 0. \quad (5.17)$$

The five unknown amplitudes $\hat{p}_0 A_1$, $\hat{p}_0 A_2$, $\hat{p}_0 A_p$, $\hat{p}_0$ and $\hat{\eta}$ satisfy the five homogeneous equations (5.9), (5.13), (5.14), (5.16) and (5.17). To obtain a non-trivial solution the determinant of the above-mentioned set of homogeneous equations should be zero, which yields the characteristic equation for the semi-infinite tethered, initially stressed, orthotropic, viscoelastic tube:

$$\begin{aligned} k'^4(1-F)\,B' + k'^2[(B'_{21}+B'_{12}-\tfrac{1}{2}B'_{11})\,F + B'_{11}(1-F)\,K - 2B'_{22}] + F - 2K \\ +\tfrac{1}{4}\exp\left\{\frac{\mathrm{i}\omega a}{c_0}\frac{x}{a}k'\right\}\left[2k'^2(F+2B'_{TS})(FB'_{11}-2B'_{12})\cos\left\{\frac{\omega a}{c_0}\frac{x}{a}\delta_1\right\}\right. \\ -\mathrm{i}k'(FB'_{11}-2B'_{12})\left\{(F-2K)\frac{FB'_{11}}{B'}-\frac{4B'_{12}}{B'_{11}}\right\}\delta_1\sin\left\{\frac{\omega a}{c_0}\frac{x}{a}\delta_1\right\} \\ -2\{(FB'_{11}-2B'_{12})(F-2K)(B'_{12}+B'_{11}B'_{TS})/B'\}\cos\left\{\frac{\omega a}{c_0}\frac{x}{a}\delta_1\right\} \\ \left. +2(F+2K)\frac{B'_{11}B'_{12}B'_{TS}}{B'}\right] = 0. \end{aligned} \quad (5.18)$$

The characteristic equation (5.18) involves x, which is usually not present in a dispersion equation. One would expect a dependence on x, as the wall displacements depend on x, and therefore, of the five amplitudes $\hat{p}_0 A_1$, $\hat{p}_0 A_2$, $\hat{p}_0 A_p$, $\hat{p}_0$ and $\hat{\eta}$, $\hat{\eta}$ is a slowly varying function of x. The first four terms in (5.18) are independent of x/a and are the same as the dispersion equation for the unbounded tube. The dispersion equation for the semi-infinite tube is no longer a relatively simple quadratic equation in k'^2, but a complicated transcendental equation. To obtain the roots, Cauchy's formulae of complex-function theory are used. The method is documented by McCune (1966). He discusses how the zeros and poles of an analytic function may be determined within some contour in the complex plane. A subroutine using this method has been programmed by Beasley & Meier (1974) and further improved by Giri & Baum (1978). The method is applied over a square contour, where also the two roots for the unbounded tube are found which represent the travelling waves of this tube.

The dispersion equation (5.18) shows that k' depends on many parameters: the parameters that describe the properties of the wall and the surrounding tissues, the radius of the tube, the properties of the fluid, the frequency of the pulsation, the initial strains applied on the tube, and the axial distance from the fixed point. In the following discussion, particularly the variation of the dimensionless phase velocities and decrement will be considered as functions of the dimensionless axial distance x/a from the fixed point. We will restrict ourselves to an elastic tube with a reference phase velocity c_0 of 5 m/s, a Poisson ratio σ of 0.5 and no surrounding tissues. tethering constants Z_{11}, L_1 and M_1 are therefore taken to be zero and K reduces to $-\rho_w h/\rho a$. The liquid is Newtonian, so only real values of the frequency parameter α are considered.

6. Discussion of the results for the semi-infinite tube

The results for the bounded tube are shown for the Young mode in the figure 6 and for the Lamb mode in figure 7. The figures show the variation of the dimensionless phase velocity (6*a*, 7*a*) and the decrement (6*b*, 7*b*) as functions of the dimensionless axial distance x/a from the fixed point at $x = 0$ of the tube. Figure 6(*a*) shows the variation of the phase velocity with x/a for $K = -0.1$, $T' = S' = 0$ and for $\alpha = 10$, 35 and 60 respectively. As in the case of the unbounded tube the phase velocity varies

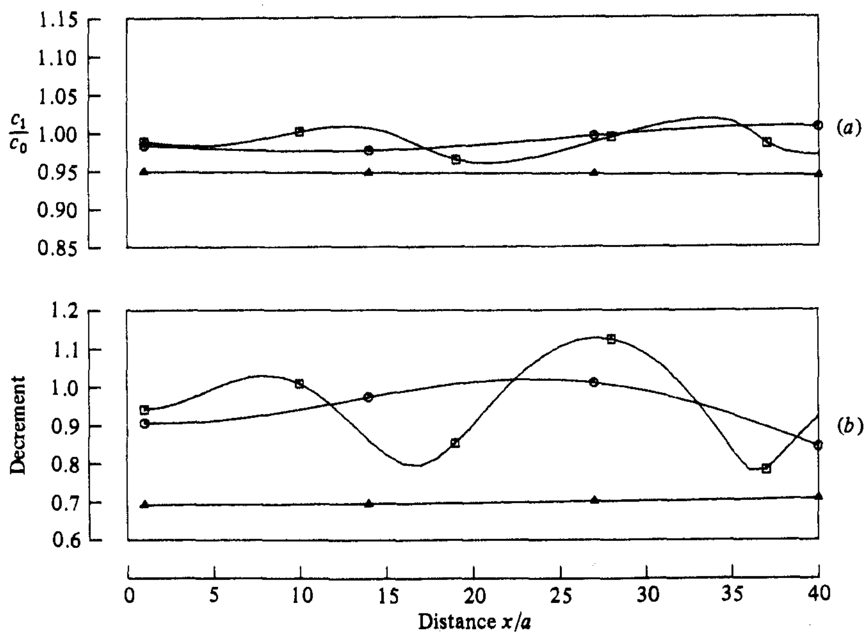

FIGURE 6. Dimensionless phase velocity c_1/c_0 and the decrement $\exp(k_1)$ for the Young mode as functions of the dimensionless distance x/a for $K = -0.1$, $T' = S' = 0$ for three values of the frequency parameter α: □, $\alpha = 60$; ○, 35; △, 10.

only slightly for $\alpha > 5$. For $\alpha = 10$ it varies also slightly with x/a, that is from 0.950 for $x/a = 1$ to 0.943 for $x/a = 40$, whereas the unbounded-tube solution gives 0.958. The variation with x/a increases with α, up to 4 % for $\alpha = 60$, and it increases also with the mass of the tube wall, e.g. for $K = -0.2$ the variation with x/a is 6 %. The variations are always within this value for the Young mode. For $B'_{12} = 0$, that is for $T' = 0.5$, the indirect constitutive equation for the radial wall displacement η becomes a direct one, the variations become practically independent of x/a with $c_1/c_0 = 1.141 \pm 0.001$, which can be compared with the unbounded-tube value 1.141.

The variation of the decrement $\exp(-k_1)$ with distance is more pronounced than the variation of the phase velocity with distance. In figure 6(*b*) it is seen again that for lower values of α the variation is small but increases progressively with α. Evidently for large α amplification of a disturbance is possible. For $\alpha = 60$, $T' = S' = 0$, $K = -0.1$ the variations are between 0.815 at $x/a = 18$ and 1.128 at $x/a = 27$, the decrement in the infinite tube being 0.959. Following the behaviour of the first mode with distance we notice that the amplitude firstly decreases slightly, and then is amplified; this is followed by a significant attenuation, which decreases passing again into an amplification of the first mode's amplitude. This pattern seems to be repeated with distance. The final effect is that the mode propagates through the tube in a manner comparable to the propagation inferred from the infinite tube; however, the amplitude does not decrease monotonically. For $B'_{12} = 0$ this behaviour disappears and the variation of the transmission per wavelength with distance becomes negligible, 0.9304 ± 0.0002, while the infinite tube yields 0.9271. It should be noted that for $B'_{12} = 0$ the extra terms appearing in (5.18) for the bounded tube have a common factor FB'_{11}. For large α this is a small factor. For the lower values of α or for $B'_{12} = 0$ it can be concluded that the variations with x/a are very limited for the Young mode. The same conclusion holds for the Lamb mode. The Lamb-mode phase velocity c_2/c_0 for $\alpha = 10$ increases slightly from 3.36 at $x/a = 1$ to 3.40 at $x/a = 40$, with a variation in the decrement from 0.312 to 0.322. The phase velocity is lower than the value for the infinite tube, 3.80, while the transmission is higher for the bounded tube than for the unbounded tube, being 0.257. For $\alpha = 35$ the phase velocities of the Lamb mode are larger and also increase almost linearly with the distance from 4.08 to 4.85, while the infinite-tube value is 4.68. The decrement for $\alpha = 35$ varies with distance from 0.610 at $x/a = 1$ to 0.552 at $x/a = 40$. The tendencies noticed at $\alpha = 35$ become more pronounced at $\alpha = 60$. Figure 7 (*a*) shows that for $K = -0.1$ and $T' = S' = 0$ the phase velocity of the second mode increases strongly with distance, but figure 7 (*b*) shows that the wave becomes practically non-propagating for $x/a > 29$. However, a third mode is found which becomes propagating for $x/a > 29$. The phase velocity increases linearly from 3.71 at $x/a = 35$ to 4.57 at $x/a = 53$, where the decrement is increased to 0.959. This may explain the experimental results of Anliker *et al.* (1968), who measured the axial wall motion of the carotid artery with heart beat at different distances from the heart and found that the higher harmonics were strongly damped with distance. The measurements of van Citters (1960) are also consistent with the above tendencies shown for the Lamb mode. Van Citters showed that the axial wave in a Penrose tube of a length of 1 m could easily be suppressed by manual constriction of the tube, that is by introducing an axial constraint. Figure 7 (*b*) shows further that the increase in damping with distance from $x/a = 6$ to $x/a = 30$ disappears for $B'_{12} = 0$. This may account for the fact (McDonald 1974) that the axial wave is sometimes observed and sometimes not. Moreover the axial displacements of the wall for bounded tubes are finite for $\omega \to 0$ and $x < \infty$, while for the unbounded tube it is of the order $1/\omega$. The difference illustrates the fact that with an axial constraint at a point there is strain energy involved in stretching the tube owing to the forces exerted by the fluid on the wall, which is absent in the analysis of the unbounded tube. Not shown in figure 7 are two other modes for $B'_{12} \neq 0$ having a phase velocity of the order of the first mode but a decrement some ten times smaller. These extra modes become non-propagating when $B'_{12} = 0$.

From figures 6 and 7 as well as from the dispersion equation for the bounded tube (5.18) it can be concluded that for $B'_{12} \neq 0$ the indirect constitutive equation for η is of influence for all values of x/a. It is finally noted that when the tube is stiff in axial direction, hence $E_x \to \infty$ and hence $\sigma_\theta \to 0$, $B'_{22} \to \infty$, $B'_{11} = 2$, the dispersion formula for the bounded tube (5.18) reduces to the simple dispersion of Kerris (1939) $k'^2 = 1/(1-F)$ for the unbounded tube.

7. Conclusions

The initial diastolic pressure in human arteries implies that $B'_{21} \sim 0$. It is discussed whether for this value of B'_{21} the axial displacements of the wall can be neglected so that the radial displacements of the wall are almost completely determined by the amplitude of the pressure pulse alone.

The influence of an initial boundary condition of the axial tube-wall displacement is in particular significant for the attenuation. The variation with the axial distance is caused by the interaction of the radial displacement with the axial displacement. The latter varies with distance to the point of fixation of the tube wall. It is shown that for an elastic tube without prestresses the variation of the attenuation of the Young mode along the tube decreases with the decrease of the frequency parameter.

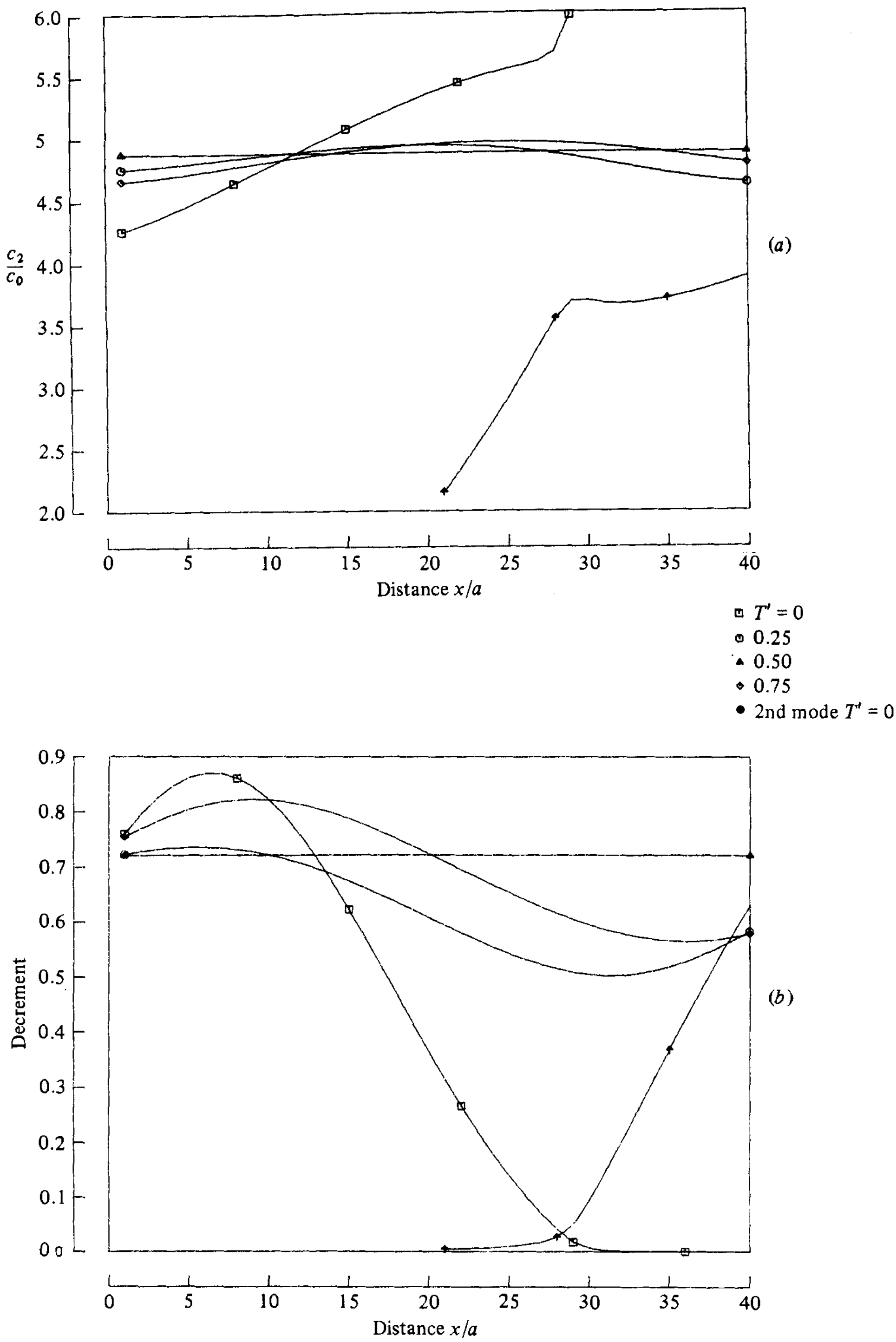

FIGURE 7. (*a*) Dimensionless phase velocity c_2/c_0 of the Lamb mode as a function of the dimensionless distance x/a for $\alpha = 60$, $K = -0.1$ and for four values of the circumferential strain T'. (*b*) Decrement $\exp(-k_2)$ of the Lamb mode as a function of the dimensionless distance x/a for the same values as in (*a*).

The phase velocity of the Young mode varies slowly along the tube, and its numerical value is quite well approximated by the simple dispersion equation of Womersley.

The Lamb mode, which is primarily associated with the axial tube-wall motions, is strongly determined by prevention of the axial wall motion at some point. The obtained results for this mode are consistent with measurements.

The author would like to thank referees for their suggestions and criticism, Mr P. G. Duijnkerke for pinpointing an error in an earlier version of the manuscript, and Mr A. Tijhuis and Professor A. T. de Hoop for the use of software developed in the Laboratory of Electromagnetic Research.

REFERENCES

ANLIKER, M., MORITZ, W. E. & OGDEN, E. 1968 Transmission characteristics of axial waves in blood vessels. *J. Biomech.* **1**, 235–246.

ATABEK, H. B. 1968 Wave propagation through a viscous fluid contained in a tethered, initially stressed, orthotropic elastic tube. *Biophys. J.* **8**, 626–649.

ATABEK, H. B. & LEW, H. S. 1966 Wave propagation through a viscous incompressible fluid contained in an initially stressed elastic tube. *Biophys. J.* **6**, 481–503.

BEASLEY, C. O. & MEIER, H. K. 1974 Subroutine Cauchy: complex roots of a function using a Cauchy integral technique. *Oak Ridge, Tennessee, Maths Note* no. 37.

CITTERS, R. L. VAN 1960 Longitudinal waves in the walls of fluid-filled elastic tubes. *Circ. Res.* **8**, 1145–1148.

FLAUD, P., GEIGER, D., ODDOU, C. & QUÉMADA, D. 1974 Écoulements pulsés dans les tuyaux viscoélastiques. Application à l'étude de la circulation sanguine. *J. Phys.* (*Paris*) **35**, 869–882.

FLAUD, P., GEIGER, D., ODDOU, C. & QUÉMADA, D. 1975 Experimental study of wave propagation through viscous fluid contained in viscoelastic cylindrical tube under static stresses. *Biorheol.* **12**, 347–354.

FLÜGGE, W. 1973 *Stresses in Shells*, 2nd edn. Springer.

GIRI, D. V. & BAUM, C. E. 1978 Application of Cauchy's residue theorem in evaluating the poles and zero's of complex meromorphic functions and apposite computer programs. *Berkeley Maths Note* no. 55.

GROOT, S. R. DE, & MAZUR, P. 1962 *Non-Equilibrium Thermodynamics*. North-Holland.

HELMHOLTZ, H. VON 1863 *Verhandlungen der Naturhistorisch-Medizinischen Vereins zu Heidelberg*, Band III, p. 16.

IBERALL, A. S. 1950 Attenuation of oscillatory pressures in instrument lines. *US Dept Commerce, Res. Paper* RP 2115; *J. Res. Natl Bur. Stand.* **45**, 85–108.

KERRIS, W. 1939 Einfluss der Rohrleitung bei der Messung periodisch schwankender Drücke. *Zentralblatt für Wissenschaftliches Berichtwesen, Berlin–Adlerhof* F.B. 1140.

KIRCHOFF, G. 1868 Ueber den Einfluss der Wärmeleitung in einem Gase auf die Schallbewegung. *Poggendorfer Ann.* **134**, 177–193.

KOITER, W. T. 1967 General equations of elastic stability for thin shells. In *Proc. Symp. on the Theory of Shells to honour L. H. Donnell, 4–6 April 1966, Houston, Texas*, pp. 187–227. University of Houston.

KORTEWEG, D. J. 1878 Über die Fortpflanzungesgeschwindigkeit des Schalles in elastischen Röhren. *Ann. Phys. Chem., Neue Folge* **5**, 525–542.

KUIKEN, G. D. C. 1984 Approximate dispersion equations for thin wall liquid filled tubes. *Appl. Sci. Res.* **41**, 37–53.

LIGHTHILL, M. J. 1970 Possible time-lag of mechanical origin following relief of venous congestion. Appendix to Caro, G. G., Foley, T. H. & Sudlow, M. F. 'Forearm vasodilatation following release of venous congestion'. *J. Physiol.* **207**, 257–269.

MCCUNE, J. E. 1966 Exact inversion of dispersion relations. *Phys. Fluids* **9**, 2082–2084.

MCDONALD, D. A. 1974 *Blood Flow in Arteries*, 2nd edn. Arnold.

MAXWELL, J. A. & ANLIKER, M. 1968 The dissipation and dispersion of small waves in arteries and veins with viscoelastic wall properties. *Biophys. J.* **8**, 920–950.

MOENS, A. I. 1878 *Die Pulskurve*. Brill, Leiden.

MOODIE, T. B., HADDOW, J. B. & TAIT, R. J. 1982 Wave propagation in a thin walled fluid filled viscoelastic tube. *Acta Mech.* **42**, 123–134.

PATEL, D. J. & VAISHNAV, R. N. 1972 The rheology of large blood vessels. In *Cardiovascular Fluid Dynamics* (ed. D. H. Bergel), ch. 11. Academic.

PEDLEY, T. J. 1980 *The Fluid Mechanics of Large Blood Vessels*. Cambridge University Press.

RAYLEIGH, LORD 1896 *Theory of Sound*, vol. II, 2nd edn, pp. 319–326. Macmillan.

RUBINOW, S. I. & KELLER, J. B. 1971 Wave propagation in a fluid-filled tube. *J. Acoust. Soc. Am.* **50**, 198–223.

WOMERSLEY, J. R. 1955 Oscillatory motion of a viscous liquid in a thin-walled elastic tube – I: The linear approximation for long waves. *Phil. Mag.* **46**, 199–221.

YARON, I. & GAL-OR, B. 1974 Similarity rules and degrees of thermodynamic coupling in flowing systems. *Appl. Sci. Res.* **30**, 17–31.

YOUNG, T. 1808 Hydraulic investigations, subservient to an intended Croonian lecture on the motion of blood. *Phil. Trans. R. Soc. Lond.* **98**, 164–186.

ZWIKKER, C. & KOSTEN, C. 1949 *Sound Absorbing Materials*. Elsevier.